Short Note

1-(3-(2-(Dimethylammonio)ethyl)-1H-indol-5-yl)- N-Methylmethanesulfonamide Succinate Hemi(Ethanol Solvate)

Petr A. Buikin , Anna V. Vologzhanina , Alexander A. Korlyukov *

Posted Date: 13 December 2023

doi: 10.20944/preprints202312.1010.v1

Keywords: active pharmaceutical ingredient; H-bond propensity; single-crystal X-ray diffraction; sumatriptan

Short note

1-(3-(2-(Dimethylammonio)ethyl)-1H-indol-5-yl)-N-Methylmethanesulfonamide Succinate Hemi(Ethanol Solvate)

Petr A. Buikin [1,2], Anna V. Vologzhanina [1] and Alexander A. Korlyukov [1,*]

[1] A. N. Nesmeyanov Institute of Organoelement Compounds, Russian Academy of Sciences, 28 Vavilov St., Moscow 119334, Russia; vologzhanina@mail.ru
[2] N.S. Kurnakov Institute of General and Inorganic Chemistry, Russian Academy of Sciences, 31 Leninskii prosp., Moscow 119991, Russia; peterzzz@mail.ru
* Correspondence: alex@xray.ineos.ac.ru

Abstract: Sumatriptan is a serotonin receptor agonist approved by FDA in 1992 to treat migraines. Its' solid form used in commercially available drugs Imitrex, Treximet, Onzetra Xsail and Zembrace symtouch is sumatriptan succinate. Herein we report on crystal structure of sumatriptane succinate hemi(ethanol solvate), $HSum^+ \cdot HSucc^- \cdot 0.5EtOH$, its comparison with previously reported solids containing derivatives of sumatriptan.

Keywords: active pharmaceutical ingredient; H-bond propensity; single-crystal X-ray diffraction; sumatriptan

1. Introduction

Sumatriptan succinate ($HSum^+ \cdot HSucc^-$) is the pharmaceutical active ingredient of commercially available drugs *Imitrex, Treximet* and others used to treat migraine headaches and cluster headaches. In addition, its anti-inflammatory properties were also reported [1]. The corresponding free base Sumatriptan (Sum) like all triptanes acts as serotonin 5-HT1B/5-HT1D receptor agonist [2,3]. During its metabolism Sum transform to glucuronide of indol-3-yl-acetic acid derivative via several steps [4]. The crystal structures of both Sum and $HSum^+ \cdot HSucc^-$ were published before [5,6].

Taking into account strong effect of solvent molecules on properties of solids, such as solubility, tabletability, stability and others, pharmaceutical industry is highly interested in crystal structures of all solid forms of active pharmaceutical ingredients which can occur upon drug production. This information is required for phase identification and purity control. In our study of novel solid forms of known active pharmaceutical ingredients [7–10], the ability of sumatriptan succinate to form various solvates was examined. Recrystallization from ethanol afforded hemisolvate, $HSum^+ \cdot HSucc^- \cdot 0.5EtOH$ (**1**). Herein we report on the molecular and crystal structures of **1**, Scheme 1.

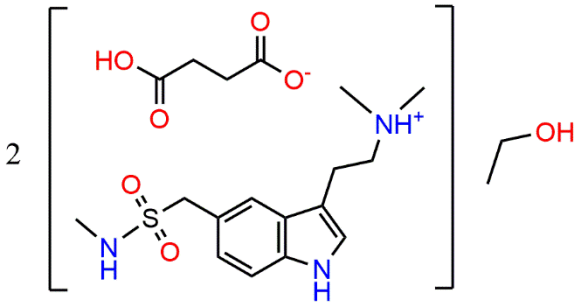

Scheme 1. Schematic representation of the title compound.

2. Results and Discussion

Sumatriptane succinate purchased from Sigma Aldrich was dissolved at ethanol without purification. After several days of standing on air at r.t. orange prismatic crystals precipitated. The

Preprints (www.preprints.org) | NOT PEER-REVIEWED | Posted: 13 December 2023 doi:10.20944/preprints202312.1010.v1

precipitate was filtered off and studied using single-crystal X-ray diffraction. The asymmetric unit of **1** is represented on Figure 1. It contains two cations, two anions, and one ethanol molecule. The positions of H(C), H(N) and H(O) can be easily revealed from difference Fourier maps. Thus, protonation of dimethylamine moiety of Sum and deprotonation of only one of two carboxylic groups of Succ was observed for all symmetrically independent species. Our conclusion about positions of hydrogen atoms is supported by interatomic and intermolecular distances. Particularly, C–O distances for deprotonated carboxylic groups vary from 1.238(4) to 1.274(4) Å. These values are intermediate between C=O and C–O(H) bond lengths for protonated groups in **1** equal to, respectively, 1.207(4) – 1.210(4) and 1.313(4) – 1.315(4) Å.

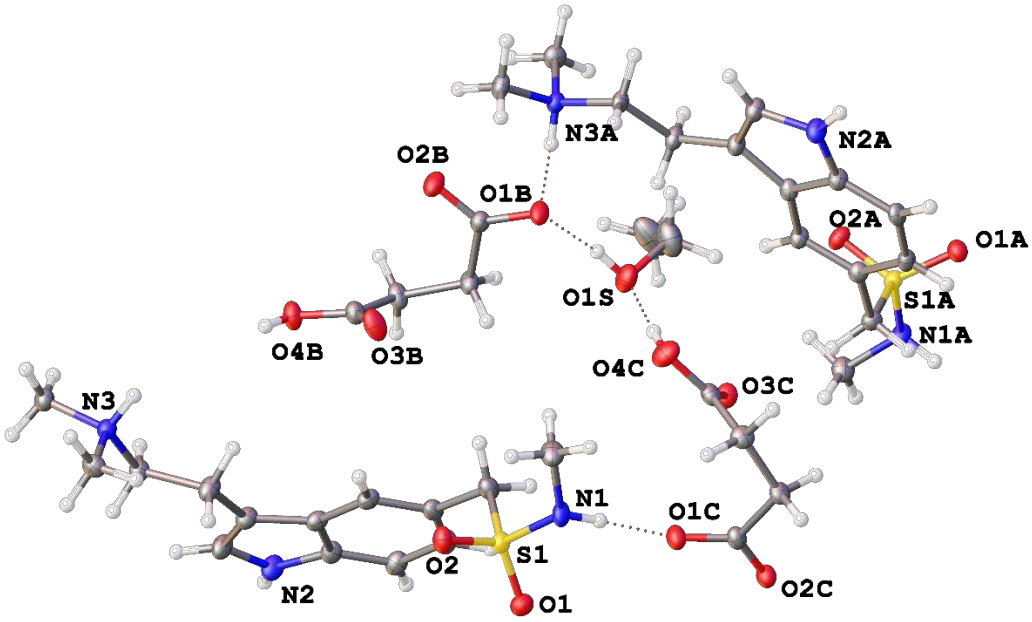

Figure 1. Asymmetric unit of **1** in representation of atoms with thermal ellipsoids (p = 50%).

Molecular conformations of cations in **1** are nearly identical with average R.M.S.D for non-hydrogen atoms equal to 0.069 Å. On Figure 2 Sum conformations in different solid forms are compared by superimposing of non-hydrogen atoms of the bicycle. It is clearly seen that rotation along single C–C, S–N and C–N groups is possible so that disposition of dimethylammonioethyl (dimethylaminoethyl) and N-methylmethanesulfonamide groups in all solids is different. Staggered conformation of succinate anions in two solvatomorphs is nearly equal: maximal deviation of non-hydrogen atoms is 0.639 Å only; the C–C–C–C torsion angle is c.a. 60°.

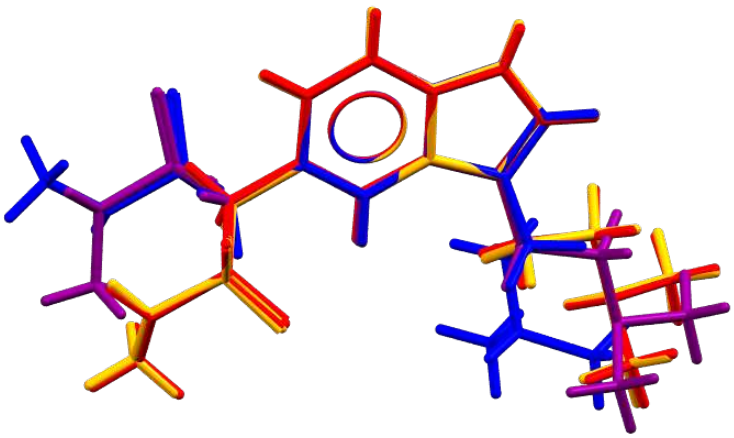

Figure 2. Molecular conformations of Sum and HSum+ in **1** (red and orange), $HSum^{+}{\cdot}HSucc^{-}$ (blue) and pure Sum (purple). Non-hydrogen atoms of the bicycle are superimposed.

Preprints (www.preprints.org) | NOT PEER-REVIEWED | Posted: 13 December 2023 doi:10.20944/preprints202312.1010.v1

Different cation conformation should be associated with different H-bonded motifs. Both in Sum and in $HSum^+ \cdot HSucc^-$ salts the number of H-bond donors and acceptors is inequivalent, thus, different functional groups compete each other to form the most stable H-bonding pattern. What is more, presence of a solvent molecule in this case is expected only if propensity of H-bond formation with this solvent is comparable or higher that propensity of H-bond formation between functional groups of main components [11]. Propensities of H-bond formation for functional groups present in $HSum^+ \cdot HSucc^-$ salts with and without ethanol were estimated using H-bond Propensities tool of Mercury package [12] as described in Refs. [13,14]. The data obtained are listed in Table 1.

Table 1. Propensities of H-bonding in $HSum^+ \cdot HSucc^-$ salts.

$HSum^+ \cdot HSucc^-$ [6]				**$HSum^+ \cdot HSucc^- \cdot 0.5EtOH$**			
Donor	**Acceptor**	**Propensity**	**Observed**	**Donor**	**Acceptor**	**Propensity**	**Observed**
R-COOH	CO_2	0.85	Yes	R-COOH	CO_2	0.84	Yes
	SO_2	0.51			SO_2	0.46	
	COOH	0.33			COOH	0.26	
					R-OH	0.34	Yes
Ammonium R_3NH^+	CO_2	0.90	Yes	Ammonium R_3NH^+	CO_2	0.81	Yes
	SO_2	0.63			SO_2	0.43	
	COOH	0.43			COOH	0.23	
					R-OH	0.31	
Indole NH	CO_2	0.97	Yes	Indole NH	CO_2	0.87	
	SO_2	0.88			SO_2	0.52	
	COOH	0.79			COOH	0.31	Yes
					R-OH	0.40	
Sulfonamide SO_2NH	CO_2	0.92	Yes	Sulfonamide SO_2NH	CO_2	0.91	Yes
	SO_2	0.68			SO_2	0.62	
	COOH	0.50			COOH	0.40	
				ROH	CO_2	0.84	Yes
					SO_2	0.47	
					COOH	0.26	
					R-OH	0.34	

The propensities evaluated indicate that in pure $HSum^+ \cdot HSucc^-$ all donors take part in H-bonding with the most likely acceptors. Presence of ethanol molecule becames possible because it is as likely donor of H-bond as COOH and R_3NH groups. In $HSum^+ \cdot HSucc^- \cdot 0.5EtOH$ two unlikely H-bonds are present, thus more stable polymorphs of this salt can exist. Fragments of experimentally obtained H-bonded networks in these two salts are compared in Figure 3. Parameters of H-bonds in solid $HSum^+ \cdot HSucc^- \cdot 0.5EtOH$ are listed in Table 2.

Table 2. Hydrogen bonding parameters for $HSum^+ \cdot HSucc^- \cdot 0.5EtOH$ (Å, °).

	D—H···A	**D—H**	**H···A**	**D···A**	**D—H···A**
1	N(1)–H(1)···O(1C)	0.90(2)	1.95(3)	2.844(4)	173(5)
2	N(2)–H(2)···O(3B^{i})	0.89(2)	2.06(3)	2.877(5)	151(1)
3	N(3)–H(3)···O(2C)	0.89(2)	1.81(3)	2.668(4)	162(4)
4	N(1A)–H(1AA)···O(2B^{ii})	0.87(2)	1.95(3)	2.794(4)	163(4)
5	N(2A)–H(2AA)···O(3C^{iii})	0.89(2)	2.06(3)	2.877(5)	151(1)
6	N(3A)–H(3A)···O(1B)	0.88(2)	1.80(3)	2.636(4)	158(6)
7	O(4C)–H(4C)···O(1S)	0.86(2)	1.68(2)	2.532(4)	170(4)

Preprints (www.preprints.org) | NOT PEER-REVIEWED | Posted: 13 December 2023 doi:10.20944/preprints202312.1010.v1

	D—H···A	D—H	H···A	D···A	D—H···A
8	O(1S)–H(1S)···O(1B)	0.85(2)	1.78(3)	2.602(4)	163(5)
9	O(4B)–H(4B)···O(2C^{iii})	0.84(2)	1.70(3)	2.526(3)	165(3)

Symmetry codes: (i) 1+x,y,z; (ii) x,-1+y,z; (iii) -1+x,y,z.

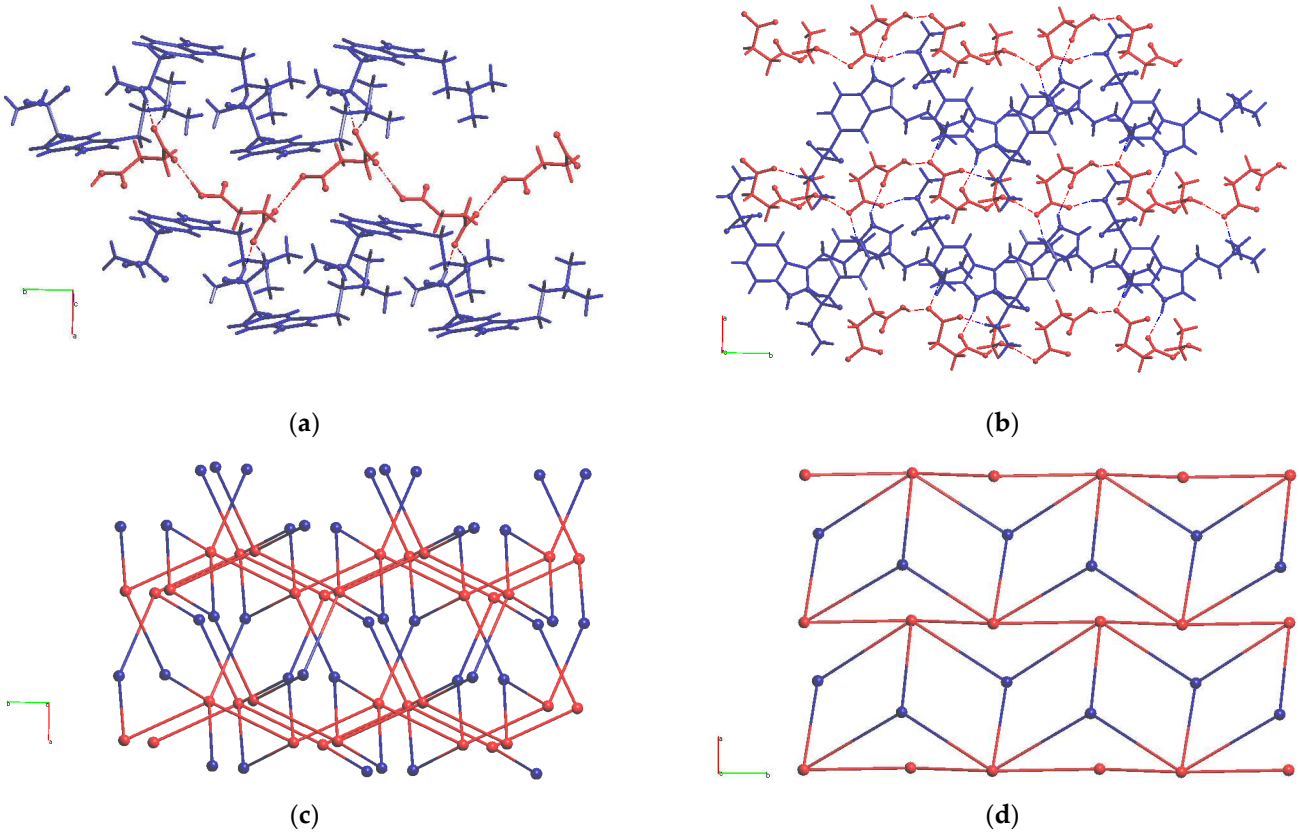

Figure 3. Fragment of H-bonded motifs in (a) HSum$^+$·HSucc$^-$ [6], (b) HSum$^+$·HSucc$^-$·0.5EtOH. HSum+ and HSucc– ions are marked with blue and red, respectively. H-bonds are dashed. (c, d) Underlying H-bonded nets in the same salts.

HSucc$^-$ anions form infinite chains in HSum$^+$·HSucc$^-$ [6] in accord with the most likely H-bonds (red chains in Fig. 3, a). In HSum$^+$·HSucc$^-$·0.5EtOH ethanol molecules act as linkers within similar chains (red chains in Fig. 3, b). HSum$^+$ cations connect these chains into infinite frameworks and layers, respectively. In both solids, the cation acts as a three-connected node of H-bonded network, and the anion is a five-connected node. The resulting topologies of underlying 3,5-c binodal H-bonded nets in these compounds evaluated with the ToposPro package [15] are, respectively, seh-3,5-P2$_1$/c and 3,5L24 (for notation of nets see Ref. [16]).

To sum up, by recrystallization from ethanol we obtained a novel solid form of sumatriptan succinate used to treat migraine and cluster headaches. Co-crystallization with ethanol is in accord with the most likely H-bonds in a three-component mixture as estimated using H-bond propensity tool, because the propensities of OH…O$_2$C and COOH…O$_2$C bonds were found to be similar. In both solids the cations and anions act as three- and five-connected nodes, and ethanol molecules – as simple linkers between two anions. Nevertheless, presence of solvent molecules strongly affects overall H-bonding network. In pure HSum$^+$·HSucc$^-$ 3D H-bonded framework is observed, while in HSum$^+$·HSucc$^-$·0.5EtOH 2D layers are found.

3. Materials and Methods

Fine powder of sumatriptane succinate (0.012 g, 0.0046 mmol) was dissolved in 3 ml of water-ethanol mixture. Single crystals were grown by slow evaporation. NMR spectra were obtained for ^{1}H at 400 MHz, for ^{13}C at 100 MHz and for ^{15}N at 40 MHz, using Bruker AVANCE III WB 400

spectrometer (Bruker, Billerica, MA, USA). FTIR spectrum was recorded on an IR spectrometer with a Fourier transformer Shimadzu IRTracer100 (Kyoto, Japan) in the range of 4000–600 cm^{-1} at a resolution of 1 cm^{-1} (Nujol mull, KBr pellets).

3.1. X-Ray diffraction

The intensities of reflections were collected at Centre for Molecular Studies of INEOS RAS with Bruker D8 QUEST diffractometer at 100K (MoKα = 0.71072 Å, φ and ω-scans). The structure was solved by the dual-space algorithm [17] and refined by full-matrix least squares against F^2 as two component inversion twin (SHELXL program [18]) using OLEX2 package [19], scale factors for two components are equal to 0.32(7) and 0.68(7), respectively. Non-hydrogen atoms were refined in an anisotropic approximation. Hydrogen atoms at carbon ones were calculated and included in the refinement with $U_{iso}(H) = 1.2U_{eq}(C)$. Hydrogen atoms of N-H and O-H groups were located in difference Fourier maps and refined with unconstrained U_{iso} and fixed bond distances (0.88 and 0.85Å, respectively).

Crystal Data for $C_{38}H_{60}N_6O_{13}S_2$ (M = 873.04 g/mol): monoclinic, space group Pc (no. 7), a = 9.834(9), b = 12.609(10), c = 16.946(16) Å, α = 90, β = 90.94(3), γ = 90°, V = 2101(3) $Å^3$, Z = 2, μ = 0.198 mm^{-1}, D_{calc} = 1.380 g cm^{-3}, F(000) = 932, 22256 reflections measured (4.0° ≤ 2Θ ≤ 61.8°), 10388 unique (R_{int} = 0.0602, R_{sigma} = 0.0763) which were used in all calculations. The final R_1 was 0.0467 ($I > 2\sigma(I)$) and wR_2 was 0.1188 (all data).

Supplementary Materials: The following supporting information can be downloaded at the website of this paper posted on Preprints.org. crystallographic data in Crystallographic Information File (CIF) format..

Author Contributions: Conceptualization, A.A.K.; methodology, P.A.B.; investigation, A.V.V. and P.V.D.; writing—A.A.K. and A.V.V.; funding acquisition, A.A.K. All authors have read and agreed to the published version of the manuscript.

Funding: This research was funded by the Russian Science Foundation, grant number 20-13-00241.

Data Availability Statement: The X-ray data are available at CCDC under ref. code CCDC 2306805.

Acknowledgments: Ministry of Science and Higher Education of the Russian Federation is acknowledged for providing access to scientific literature.

Conflicts of Interest: The authors declare no conflict of interest.

References

1. Ala, M.; Ghasemi, M.; Mohammad Jafari, R.; Dehpour, A.R. Beyond Its Anti-Migraine Properties, Sumatriptan Is an Anti-Inflammatory Agent: A Systematic Review. *Drug Dev. Res.* **2021**, *82*, 896–906, doi:10.1002/ddr.21819.
2. Syed, Y.Y. Sumatriptan/Naproxen Sodium: A Review in Migraine. *Drugs* **2016**, *76*, 111–121, doi:10.1007/s40265-015-0521-8.
3. Tfelt-Hansen, P.; De Vries, P.; Saxena, P.R. Triptans in Migraine. *Drugs* **2000**, *60*, 1259–1287, doi:10.2165/00003495-200060060-00003.
4. Pöstges, T.; Lehr, M. Metabolism of Sumatriptan Revisited. *Pharm. Res. Persp.* **2023**, *11*, e01051, doi:10.1002/prp2.1051.
5. Ravikumar, K.; Sridhar, B.; Krishnan, H. Sumatriptan, an Anti-migraine Drug. *Acta Cryst., Sect. E* **2006**, *62*, o1086–o1088, doi:10.1107/S1600536806005101.
6. Ravikumar, K.; Swamy, G.Y.S.K.; Krishnan, H. α-{3-[2-(Di-methyl-ammonio)-ethyl]-1H-Indol-5-Yl}-N-Methyl-methanesulfon-amide Succinate (Sumatriptan Succinate). *Acta Cryst., Sect. E* **2004**, *60*, o618–o620, doi:10.1107/S1600536804005896.
7. Goloveshkin, A.S.; Korlyukov, A.A.; Vologzhanina, A.V. Novel Polymorph of Favipiravir—An Antiviral Medication. *Pharmaceutics* **2021**, *13*, 139, doi:10.3390/pharmaceutics13020139.
8. Korlyukov, A.A.; Dorovatovskii, P.V.; Vologzhanina, A.V. N-(4-Methyl-3-((4-(Pyridin-3-Yl)Pyrimidin-2-Yl)Amino)Phenyl)-4-((4-Methylpiperazin-1-Yl)Methyl)Benzamide. *Molbank* **2022**, *2022*, M1461, doi:10.3390/M1461.

9. Korlyukov, A.A.; Buikin, P.A.; Dorovatovskii, P.V.; Vologzhanina, A.V. Synthesis, NoSpherA2 Refinement, and Noncovalent Bonding of Abiraterone Bromide Monohydrate. *Struct. Chem.* **2023**, *34*, 1927–1934, doi:10.1007/s11224-023-02210-3.
10. Buikin, P.; Vologzhanina, A.; Novikov, R.; Dorovatovskii, P.; Korlyukov, A. Abiraterone Acetate Complexes with Biometals: Synthesis, Characterization in Solid and Solution, and the Nature of Chemical Bonding. *Pharmaceutics* **2023**, *15*, 2180, doi:10.3390/pharmaceutics15092180.
11. Delori, A.; Galek, P.T.A.; Pidcock, E.; Jones, W. Quantifying Homo- and Heteromolecular Hydrogen Bonds as a Guide for Adduct Formation. *Chem. – Eur. J.* **2012**, *18*, 6835–6846, doi:10.1002/chem.201103129.
12. Macrae, C.F.; Sovago, I.; Cottrell, S.J.; Galek, P.T.A.; McCabe, P.; Pidcock, E.; Platings, M.; Shields, G.P.; Stevens, J.S.; Towler, M.; et al. Mercury 4.0: From Visualization to Analysis, Design and Prediction. *J. Appl. Cryst.* **2020**, *53*, 226–235, doi:10.1107/S1600576719014092.
13. Galek, P.T.A.; Allen, F.H.; Fábián, L.; Feeder, N. Knowledge-Based H-Bond Prediction to Aid Experimental Polymorph Screening. *CrystEngComm* **2009**, *11*, 2634–2639, doi:10.1039/B910882C.
14. Vologzhanina, A.V. Intermolecular Interactions in Functional Crystalline Materials: From Data to Knowledge. *Crystals* **2019**, *9*, 478, doi:10.3390/cryst9090478.
15. Shevchenko, A.P.; Blatov, V.A. Simplify to Understand: How to Elucidate Crystal Structures? *Struct. Chem.* **2021**, *32*, 507–519, doi:10.1007/s11224-020-01724-4.
16. A. Blatov, V.; O'Keeffe, M.; M. Proserpio, D. Vertex-, Face-, Point-, Schläfli-, and Delaney-Symbols in Nets, Polyhedra and Tilings: Recommended Terminology. *CrystEngComm* **2010**, *12*, 44–48, doi:10.1039/B910671E.
17. Sheldrick, G.M. SHELXT – Integrated Space-Group and Crystal-Structure Determination. *Acta Cryst., Sect. A* **2015**, *71*, 3–8, doi:10.1107/S2053273314026370.
18. Sheldrick, G.M. Crystal Structure Refinement with SHELXL. *Acta Cryst., Sect. C* **2015**, *71*, 3–8, doi:10.1107/S2053229614024218.
19. Dolomanov, O.V.; Bourhis, L.J.; Gildea, R.J.; Howard, J. a. K.; Puschmann, H. OLEX2: A Complete Structure Solution, Refinement and Analysis Program. *J. Appl. Cryst.* **2009**, *42*, 339–341, doi:10.1107/S0021889808042726.